

## Crystal structure and optical properties of Na- and Pb-exchanged heulandite-group zeolites

MICKEY E. GUNTER

Department of Geology and Geological Engineering, University of Idaho, Moscow, Idaho 83844, U.S.A.

THOMAS ARMBRUSTER, THOMAS KOHLER

Laboratorium für chemische und mineralogische Kristallographie, Universität Bern, Freiestrasse 3, CH-3012 Bern, Switzerland

CHARLES R. KNOWLES

Idaho Geological Survey, University of Idaho, Moscow, Idaho 83844, U.S.A.

### ABSTRACT

Cation exchange experiments were conducted on three heulandite-group zeolites from Fiesch, Switzerland ( $\text{Ca}_{3.6}\text{K}_{0.8}\text{Al}_{8.8}\text{Si}_{27.4}\text{O}_{72} \cdot 26.1\text{H}_2\text{O}$ ); Succor Creek, Oregon ( $\text{Ca}_{2.1}\text{Mg}_{0.3}\text{Na}_{2.5}\text{K}_{0.3}\text{Al}_{8.0}\text{Si}_{28.2}\text{O}_{72} \cdot 25.5\text{H}_2\text{O}$ ); and Poona, India ( $\text{Ca}_{3.7}\text{Na}_{1.3}\text{K}_{0.1}\text{Al}_{8.9}\text{Si}_{27.1}\text{O}_{72} \cdot 21.4\text{H}_2\text{O}$ ). Only the Poona sample was completely Na and, in turn, Pb exchanged. Diffusion gradients for the other two samples were observed by both backscattered electron images and optical retardation on (010). For the Poona sample, single-crystal X-ray structure refinements of the nonexchanged, Na-exchanged ( $\text{Na}_{8.8}\text{Al}_{8.9}\text{Si}_{27.1}\text{O}_{72} \cdot 19.2\text{H}_2\text{O}$ ), and Pb-exchanged ( $\text{Pb}_{4.4}\text{Al}_{8.9}\text{Si}_{27.1}\text{O}_{72} \cdot 16.4\text{H}_2\text{O}$ ) samples were performed with resultant *R* values of 5.2, 5.7, and 8.1% in space groups *C2/m*, *C2/m*, and *Cm*, respectively. There is only one metal position in the B channel for the Pb sample, whereas this position is split for the nonexchanged and Na-exchanged samples. This, along with channel H<sub>2</sub>O locations, causes the reduction in symmetry for the Pb-exchanged sample. The framework topology remains essentially unchanged for the three samples.

The optical properties of the Poona sample were determined, and the birefringence in (010) was found to vary dramatically, ranging from 0.001 for the nonexchanged sample to 0.0145 for the Pb-exchanged sample, whereas the mean refractive indices ranged from 1.488 for the Na-exchanged sample to 1.573 for the Pb-exchanged sample.

### INTRODUCTION

Heulandite,  $(\text{Na,K})\text{Ca}_4(\text{Al}_9\text{Si}_{27}\text{O}_{72}) \cdot 24\text{H}_2\text{O}$ , and clinoptilolite,  $(\text{Na,K})_6(\text{Al}_6\text{Si}_{30}\text{O}_{72}) \cdot 20\text{H}_2\text{O}$ , are end-members of the group referred to here as the heulandite-group zeolites. There is some controversy whether clinoptilolite should be considered a separate species. Mumpton (1960) favored retaining the name, but Tschernich (1992) favored using “high-silica” heulandite. Three methods are proposed to distinguish between the two species: framework chemistry (Boles, 1972), channel occupants (Mason and Sand, 1960), and thermal stability (Mumpton, 1960). Besides chemical and thermal differences, there are petrologic differences between the two. In general, clinoptilolite forms in the sedimentary environment from altered tuffs, whereas heulandite occurs as a vesicle filling in basalts. Their structures are characterized by large, intersecting open channels of eight- and ten-membered tetrahedral rings. Two of these rings form main channels (types A and B) parallel to *c*. C channels are parallel to *a* or [102] and are also formed by eight-membered rings (Koyama and Takéuchi, 1977). In nature, the channels are predominantly occupied by Na, K, Ca, and H<sub>2</sub>O (e.g.,

Merkle and Slaughter, 1968; Alberti, 1972, 1975; Boles, 1972; Armbruster and Gunter, 1991).

Heulandite-group zeolites are important natural zeolites because of their cation-exchange properties (Mumpton, 1988). They have been used for the removal of radioactive Cs and Sr from low-level waste streams of nuclear installations (for a review of the literature, see Mumpton, 1978, and Smyth et al., 1990). Other applications exist in agriculture, in the extraction of NH<sub>4</sub><sup>+</sup> in sewage, or as dietary supplements in animal breeding. However, very little is known about the absorption and adsorption processes involved because of the scarcity of crystal structure refinements of cation-exchanged samples.

Only four structure analyses of fully exchanged heulandite-group zeolites have been reported in the literature: fully Cs-exchanged clinoptilolite (Smyth et al., 1990; Petrov et al., 1991), Ag-exchanged heulandite (Bresciani-Pahor et al., 1980, 1981), K-exchanged heulandite, and its high-temperature dehydration product (Galli et al., 1983). In addition, data exist on a partially Rb-exchanged heulandite sample (Sugiyama and Takéuchi, 1986) and a partially NH<sub>4</sub>-exchanged heulandite sample (Mortier and Pearce, 1981); however, Mortier and Pearce could not

resolve the exact  $\text{NH}_4$  positions. In the above studies, all exchanges were performed in an aqueous solution of 1–2 *M* concentration at temperatures close to 100 °C for times ranging from a few weeks to several months, with sample sizes on the order of 250  $\mu\text{m}$ , except the Cs-saturated clinoptilolite of Petrov et al. (1991), which was refined in powder form.

The goals of the present study are to produce completely Pb-exchanged heulandite using natural samples as the starting material and to characterize this material structurally and optically. The rationale of this investigation is twofold.

1. Heulandite-group zeolites have been shown to have a high affinity for Pb (Blanchard et al., 1984; Tuck and Ming, 1993); because of this, they have been useful in the removal of Pb from water and soil (Blanchard et al., 1984; Leppert, 1990; Grube and Herrmann, 1993; Tuck and Ming, 1993) and in the extraction of Pb from Pb-poisoned pigs (Pond et al., 1993). All these studies used fine-grained (submicrometer size) clinoptilolite formed in altered tuffaceous rocks, which also contained smectite and opal-CT. Deposits of such material are commercially available throughout the world. Routinely, only chemical analysis of the exchange material or solution is performed before and after the experiment. However, it is not clear to what extent Pb was adsorbed at the mineral surface or was actually absorbed in the structural cavities of the zeolite, and the interactions of the other minerals present in the sample are also not clear. It is necessary to resolve these uncertainties if widespread use of these minerals is to occur for water purification. For example, additional knowledge would be required to understand the subsequent release of Pb from the mineral.

2. Tiselius (1934) showed that hydration and dehydration of heulandite under defined partial pressure of  $\text{H}_2\text{O}$  and temperature can be quantitatively monitored by the accompanying change of optical birefringence and extinction angle on (010) crystal plates. These experiments indicated that cation diffusion kinetics may also be monitored under a polarizing microscope, provided that the cation exchange leads to a change of birefringence or extinction angle in (010) plates. Cation diffusion rates are also extremely important if these minerals are to be used in water purification. Thus, refractive indices and optical orientation of nonexchanged and exchanged samples must be known to determine if significant differences exist and can be observed.

#### EXPERIMENTAL PROCEDURE

Three heulandite-group zeolites from different locations were selected for cation-exchange experiments: Fiesch, Switzerland ( $\text{Ca}_{3.6}\text{K}_{0.8}\text{Al}_{8.8}\text{Si}_{27.4}\text{O}_{72} \cdot 26.1\text{H}_2\text{O}$ ) (Merkle and Slaughter, 1968); Succor Creek, Oregon, U.S.A. ( $\text{Ca}_{2.1}\text{Mg}_{0.3}\text{Na}_{2.5}\text{K}_{0.3}\text{Al}_{8.0}\text{Si}_{28.2}\text{O}_{72} \cdot 25.5\text{H}_2\text{O}$ ) (Armbruster and Gunter, 1991); and Poona, India ( $\text{Ca}_{1.7}\text{Na}_{1.3}\text{K}_{0.1}\text{Al}_{8.9}\text{Si}_{27.1}\text{O}_{72} \cdot 21.4\text{H}_2\text{O}$ ) (Sukheswala et al., 1974). The samples were chosen on the basis of availability and crystal size (i.e., crystals large enough for sin-

gle-crystal X-ray and optics). The crystals were crushed to 100–500  $\mu\text{m}$  and placed in 2 *M* of NaCl at 100 °C. After 4 weeks they were removed, filtered, and washed with distilled  $\text{H}_2\text{O}$ , yielding our Na-exchanged sample. Approximately half of this Na-exchanged sample was further treated in 2 *M* of lead acetate at 100 °C. After 3 weeks they were removed, filtered, and washed with distilled  $\text{H}_2\text{O}$ , yielding our Pb-exchanged samples.

Electron microprobe, SEM BSE (backscattered electron) images, and optical properties were used to measure the cation exchange. Compositions were determined by an ARL-EMX-SM electron microprobe operating at a 15-kV and 100-nA beam current and a defocused beam diameter of 20  $\mu\text{m}$ . Amelia albite was used as the standard for Na, Al, and Si; synthetic anorthite was used for Ca, orthoclase for K, and stoichiometric galena for Pb. All samples were also analyzed for Sr, Mg, and Fe and found to be below the detection level of approximately 0.1%.  $\text{H}_2\text{O}$  content was determined by structure refinements, and may be too low if all channel  $\text{H}_2\text{O}$  was not localized. Chemistry for the Succor Creek sample was taken from Armbruster and Gunter (1991), and the Fiesch  $\text{H}_2\text{O}$  content given by Merkle and Slaughter (1968) was used. Excalibr (Bloss, 1981; Gunter et al., 1988) was used to measure  $2V$  and for grain orientation for subsequent refractive index determinations by the double-variation method (Bloss, 1981; Su et al., 1987). BSE images were obtained on an AMRAY SEM with a resolution of 0.3 atomic number.

Single-crystal X-ray data for the nonexchanged, Na-exchanged, and Pb-exchanged Poona heulandite were collected at room temperature with an Enraf-Nonius CAD4 diffractometer (graphite-monochromatized  $\text{MoK}\alpha$  radiation). Cell dimensions were determined from 22 reflections with  $10^\circ < \theta < 15^\circ$ . Experimental details for data collection and structure refinements are given in Table 1. Reflections for the nonexchanged and Na-exchanged samples were collected between 0 and  $25^\circ \theta$ , with  $-21 < h < 21$ ,  $-21 < k < 21$ ,  $0 < l < 8$ , and  $-21 < h < 21$ ,  $0 < k < 21$ , and  $0 < l < 8$ , respectively. Reflections for the Pb-exchanged samples were collected between 0 and  $25^\circ \theta$ , with  $-21 < h < 21$ ,  $-21 < k < 21$ , and  $-8 < l < 8$  (whole sphere). All data were empirically corrected for absorption by using  $\psi$  scans. Data reduction, including background and Lorentz-polarization corrections, was performed using the SDP program library (Enraf-Nonius, 1983). Starting parameters for the refinement were obtained from Armbruster and Gunter (1991). The program SHELX76 (Sheldrick, 1976) was used for structure refinement, using a unit-weight weighting scheme.

#### RESULTS

The heulandite from Poona was the only sample to completely undergo Na and later Pb exchange. Only single-crystal X-ray and optical data could be collected for this sample. However, in the remaining two samples, cation diffusion was observed by BSE and optical retardation. For the nonexchanged, Na-exchanged, and Pb-ex-

**TABLE 1.** Data collection, refinement parameters, chemistry, and optical properties for nonexchanged, Na-, and Pb-exchanged samples from Poona, India

Sample name	nonexchanged	Na-exchanged	Pb-exchanged
Composition*	Ca <sub>3.7</sub> Na <sub>1.3</sub> K <sub>0.13</sub>	Na <sub>8.8</sub>	Pb <sub>4.4</sub>
Crystal size (mm)	0.40 × 0.45 × 0.20	0.28 × 0.20 × 0.15	0.50 × 0.25 × 0.10
Space group	<i>C2/m</i>	<i>C2/m</i>	<i>Cm</i>
Treatment	natural	4 weeks 2 M NaCl at 100 °C	4 weeks 2 M NaCl and 3 weeks 2 M lead acetate at 100 °C
Radiation	MoK $\alpha$	MoK $\alpha$	MoK $\alpha$
Scan type and width	3 $^{\circ}$ $\omega$	1.5 $^{\circ}$ $\omega$	1.5 $^{\circ}$ $\omega$
a (Å)	17.671(1)	17.767(2)	17.767(3)
b (Å)	17.875(7)	17.977(2)	17.917(2)
c (Å)	7.412(3)	7.422(2)	7.432(2)
$\beta$ (°)	116.39(3)	116.14(1)	116.33(2)
V (Å <sup>3</sup> )	2097.2	2133.8	2120.4
Maximum $\theta$ (°)	25	25	25
Measured reflections	4061	2089	7425
Unique reflections	1911	1863	3821
Observed reflections >3 $\sigma$	1821	1632	3342
No. of parameters	174	178	222
R (%)	5.19	5.72	8.14
R <sub>w</sub> (%)	5.53	6.14	9.65
$\alpha$	1.4986	1.4857	1.5632
$\beta$	1.4996	1.4883	1.5777
$\gamma$	1.5045	1.4889	1.5793
2Vz	48.8(4)	97.6(4)	116.3(2)
b =	Z	Z	Z
X:c =	+7 $^{\circ}$	+19 $^{\circ}$	+11 $^{\circ}$

Note:  $R = \sum |F_{\text{obs}}| - |F_{\text{calc}}| / \sum |F_{\text{obs}}|$ ,  $R_w = [\sum w(|F_{\text{obs}}| - |F_{\text{calc}}|)^2 / \sum w |F_{\text{obs}}|^2]^{1/2}$ .

\* Channel cations, whereas framework and H<sub>2</sub>O are Al<sub>8.9</sub>Si<sub>27.1</sub>·nH<sub>2</sub>O for all samples.

changed samples, observed and calculated structure factors are given in Table 2,<sup>1</sup> positional parameters and occupancies are listed in Tables 3–5,<sup>1</sup> and selected interatomic distances are summarized in Table 6.<sup>1</sup>

### The Nonexchanged sample

The composition obtained using electron microprobe analysis yielded the formula Ca<sub>3.7</sub>Na<sub>1.3</sub>K<sub>0.13</sub>Al<sub>8.9</sub>Si<sub>27.1</sub>O<sub>72</sub>·21.4H<sub>2</sub>O ( $Z = 1$ ); refractive indices,  $2V$ , and optical orientation were also determined (Table 1). In the nonexchanged Poona sample, three channel cation sites (M1, M2, and M3), as well as five H<sub>2</sub>O molecules (O13, O14, O16, O17, and O19), were found. Na prefers M1 (Fig. 1) (Armbruster and Gunter, 1991); thus, this position was refined with Na-scattering factors. Ca is concentrated in M2 (Fig. 1); thus, Ca-scattering factors were applied. In the following experiments, we used scattering factors for Na, Ca, and K, respectively, for the M1, M2, and M3 channel positions. The maximum occupancy of M2 can only be 50%, because its symmetry-equivalent position at  $-x, 0, -z$  is too close to permit occupancy of both sites (2.7 Å apart, Fig. 2). The *C2/m* refinement converged at an  $R$  value of 5.2% using anisotropic displacement parameters for framework atoms, channel cations, and channel O sites (H<sub>2</sub>O molecules).

### The Na-exchanged sample

Electron microprobe analysis gave the formula Na<sub>8.8</sub>Al<sub>8.9</sub>Si<sub>27.1</sub>O<sub>72</sub>·19.2H<sub>2</sub>O, representing fully Na-ex-

changed heulandite. With a polarizing microscope (crossed polars), the crystals showed fairly sharp extinction without zoning. Refractive indices,  $2V$ , and the optical orientation are given in Table 1. Na was assigned to the cation positions M1 (Na1), M2 (Na2), and M3 (Na3) (Fig. 1). The Na exchange led to a significant increase of the M2  $z$  coordinate (Table 4) compared with the nonexchanged sample. Na2 is 80% occupied by Na, and the distance between the symmetry-related sites M2 (at  $x, 0, z$ ) and M2' (at  $-x, 0, -z$ ) increased to 3.3 Å (2.7 Å in the natural sample); thus, both positions are occupied simultaneously (Fig. 2). Because of the similar scattering factors for Na and H<sub>2</sub>O, low concentrations of Na dispersed in the structural channels could not be resolved from H<sub>2</sub>O sites. Structure refinement in space group *C2/m* converged to an  $R$  value of 5.7%.

### The Pb-exchanged sample

Electron microprobe analysis gave the formula Pb<sub>4.4</sub>Al<sub>8.9</sub>Si<sub>27.1</sub>O<sub>72</sub>·16.4H<sub>2</sub>O; thus, this heulandite is also fully Pb exchanged. The refractive indices,  $2V$ , and the optical orientation are given in Table 1. A first data set for testing was refined in space group *C2/m*, yielding an  $R$  value of ca. 16%. This result, however, indicated an incorrect space-group assignment. Subsequently, a new data set was collected in *C1* symmetry (whole sphere). Test refinements in space group *C1* revealed a Pb position at 0.5380(4), 0, 0.1981(9) but not at  $-x, 0, -z$ , indicating the observed Pb distribution is in agreement with *Cm* and not with *C2* symmetry. Subsequent refinements were done in the acentric *Cm* space group. Thus, only one M2 position (Pb2) occurs in the B channel (Figs. 1 and 2). Also, because of the absence of a center of sym-

<sup>1</sup> A copy of Tables 2–6 may be ordered as Document AM-94-557 from the Business Office, Mineralogical Society of America, 1130 Seventeenth Street NW, Suite 330, Washington, DC 20036, U.S.A. Please remit \$5.00 in advance for the microfiche.

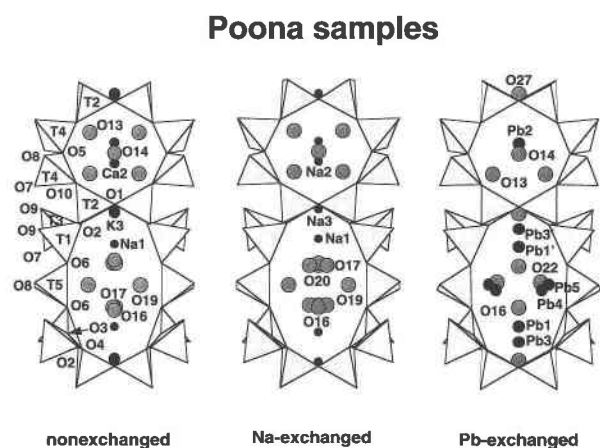


Fig. 1. Projections along [001], displaying the larger A channel confined by ten tetrahedra and the B channel confined by eight tetrahedra. Numbers refer to atom labeling in Tables 3–5 and in Armbruster and Gunter (1991, their Table 4).

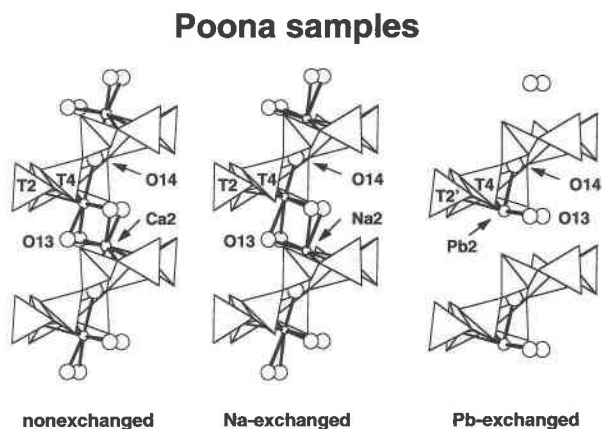


Fig. 2. Cation bonding in the B channel with *c* vertical and *a* rotated 13° out of the page.

metry, only two O13 positions occur in the B channel (Figs. 1 and 2). For atoms related by the pseudo-twofold axis (or pseudocenter of symmetry), we have adopted a prime notation. For instance, if Pb was found in both sites in the B channel, it would be denoted as Pb2 and Pb2'. The tetrahedral framework structure remained pseudocentric, with no significant differences in average T-O distances of tetrahedra related by the pseudocenter of symmetry. Thus, the symmetry reduction is mainly caused by the arrangement of Pb and H<sub>2</sub>O within the A and B channels. Additional Pb was found in the A channel in M1 and M1', M3 and M3', and close to the center (Pb4 and Pb5). Isotropic displacement parameters were applied for framework atoms, leading to an *R* value of 8.1%. Due to correlation problems (pseudocenter of symmetry), framework positions have large standard deviations.

## DISCUSSION

### The nonexchanged sample

The dominant channel cations in the nonexchanged Poona heulandite are Ca and Na with minor K (Table 1). In the structure refinement, three metal positions (Na1, Ca2, and K3) were located within the channels (Table 3, Fig. 1). Na1, located in the A channel (Fig. 1), is ninefold coordinated, with 2 × O2 (2.64 Å), 2 × O3 (3.12 Å) from the tetrahedral framework, and five strongly disordered and only partially occupied channel H<sub>2</sub>O sites: 2 × O17 (2.35 Å), 2 × O19 (2.91 Å), and O16 (2.55 Å). Ca2, located in the B channel (Figs. 1 and 2), is eightfold coordinated, with 2 × O10 (2.72 Å), O1 (2.54 Å) from the framework, and five H<sub>2</sub>O molecules: 4 × O13 (2 × 2.39 and 2 × 2.56 Å) and O14 (2.59 Å). K3, located in the C channel (Fig. 1), is eightfold coordinated, with 2 × O4 (2.91 Å), 2 × O3 (3.13 Å), and four H<sub>2</sub>O molecules: 2 × O13 (2.92 Å) and 2 × O17 (3.11 Å).

The following procedure was used to determine the populations of the channel occupants so that refined populations corresponded to microprobe results. By allowing

Ca2 to represent the Ca site, 1.94 Ca pfu satisfies the observed population of 0.484 (Table 7). This refined population of Ca2 is 1.76 pfu below the Ca value of 3.7 pfu determined by microprobe analysis. However, the population of Na1 (4.43 pfu) is significantly higher than the Na value of 1.3 pfu determined by microprobe analysis; thus, some excess Ca must be assigned to the Na1 position. By subtracting the Ca content of Ca2 (1.94 pfu) from the total Ca content (3.7 Ca pfu), a value of 1.76 Ca pfu results for Na1. Generally, the X-ray scattering power of Ca is twice that of Na; thus, one Ca atom may be considered as two Na atoms and vice versa. In contrast, the remaining population of Na in Na1 gave a value of 0.228, or 0.91 pfu. After subtracting the Na content of Na1 (0.91 Na pfu) from the total Na content (1.3 Na pfu), the remaining Na (0.39 pfu) was assigned to position K3. In addition, all K found by microprobe analysis was placed in the K3 site. The refined population of K3 is substantially higher (0.494) than the analyzed K concentration (0.13 pfu). Armbruster and Gunter (1991) reported that the K concentration in K3 is easily overestimated because of a neighboring H<sub>2</sub>O site (O11). In room temperature structure refinements, K3 and O11 cannot be easily resolved but lead to an average position with strongly anisotropic displacement parameters. Because our K3 is a mixed position between O11 and K3, we obtained a significantly higher population for this position than what was expected from microprobe analysis.

### The Na-exchanged sample

After treating the Poona sample for 4 weeks at 100 °C in a 2-*M* NaCl solution, the cell volume increased slightly (2%), accompanied by a 0.2% decrease of the  $\beta$  angle. The same channel cation positions (Na1, Na2, and Na3) as in the nonexchanged sample were refined (Table 4 and Fig. 1). Na2 is eightfold coordinated by 2 × O10 (2.73 Å) and O1 (2.56 Å) from the framework and five channel H<sub>2</sub>O molecules: 4 × O13 (2 × 2.46 and 2 × 2.86 Å) and O14 (2.30 Å) (Figs. 1 and 2). The coordination of Na1 and Na3 is poorly defined. Na1 is surrounded by O1 (2.99

**TABLE 7.** Population assignment procedure for metal content (pfu) for nonexchanged, Na-, and Pb-exchanged samples from Poona, India

Nonexchanged sample channel sites										
Cation site	Wyckoff notation	Pop. total	Pop. Ca	Ca <sup>2+</sup> (pfu)	Pop. Na	Na <sup>+</sup> (pfu)	Pop. K	K <sup>+</sup> (pfu)	Pop. H <sub>2</sub> O	
Ca2	4 i	0.484(4)	0.484	1.94	—	—	—	—	—	
Na1	4 i	1.108(8)	0.440	1.76	0.228	0.91	—	—	—	
K3	4 i	0.494(5)	—	—	0.097	0.39	0.03	0.13	0.83	
Totals (pfu)				3.70		1.30		0.13		
Na-exchanged sample channel sites					Pb-exchanged sample channel sites					
Cation site	Wyckoff notation	Pop. total	Pop. Na	Na <sup>+</sup> (pfu)	Pop. H <sub>2</sub> O	Cation site	Wyckoff notation	Pop. total	Pop. Pb	Pb <sup>2+</sup> (pfu)
Na2	4 i	0.80(2)	0.8	3.20	—	Pb2	2 a	0.60(6)	0.60	1.20
Na1	4 i	0.84(2)	0.84	3.36	—	Pb2'	vacant	—	—	—
Na3	4 i	0.84(2)	0.16	0.64	0.68	Pb1	2 a	0.32(8)	0.32	0.64
						Pb1'	2 a	0.40(8)	0.40	0.80
						Pb3	2 a	0.14(8)	0.14	0.28
						Pb3'	2 a	0.12(6)	0.12	0.24
						Pb4	4 b	0.14(6)	0.14	0.56
						Pb5	4 b	0.07(4)	0.07	0.28
Total (pfu)				7.20		Total (pfu)				4.00

Å), 2 × O2 (2.57 Å), and 2 × O3 (3.13 Å) from the framework and five strongly disordered and partially occupied channel H<sub>2</sub>O molecules: O16 (2.81 Å), 2 × O17 (2.13 Å), and 2 × O19 (3.22 Å). Na3 is coordinated by 2 × O4 (2.89 Å) and 2 × O3 (3.21 Å) from the framework and two channel H<sub>2</sub>O molecules [2 × O13 (2.84 Å)]. The shift of Na2 toward the cavity wall, compared with Ca2 in the natural sample, would allow complete occupation of the B channel by Na. This also indicates that the space group *C2/m* is correct for the Na-exchanged sample, whereas in the natural sample, *C2/m* represents only an average space group. The positional disorder in the B channel caused by the short Ca2-Ca2 distances in Ca-bearing samples allows only *Cm* symmetry locally. Similar shifts of cation positions occur in the natrolite group when Ca + H<sub>2</sub>O → 2Na, going from natrolite (Smith et al., 1984) to scolecite (Stuckenschmidt et al., 1993).

Because Na1 and Na3 are very close (2.45 Å), the sum of Na populations on Na1 and Na3 cannot exceed 1.0. Thus, in spite of the high Na3 population (0.84), only 1.28 Na pfu, or 0.16 Na, is assigned to Na3 in our model (Table 7). The remaining scattering power refined at Na3 is attributed to H<sub>2</sub>O located at the O11 site of Armbruster and Gunter (1991), which is positioned very close to Na3 and coordinates Na1. The above Na assignment to Na1, Na2, and Na3 leads to 7.20 Na pfu localized by the structure refinement (Table 7), in contrast to 8.8 Na pfu, as determined by electron microprobe analyses. The missing Na is probably positioned close to the partially occupied H<sub>2</sub>O sites O16, O17, O19, and O20. This hypothesis is supported by the large displacement parameters of these H<sub>2</sub>O positions, indicating positional disorder.

#### The Pb-exchanged sample

After the Poona sample was treated for 4 weeks at 100 °C in a 2-*M* NaCl solution and 3 weeks at 100 °C in a

2-*M* lead acetate solution, the cell volume increased slightly (1%), accompanied by a 0.1% decrease of the β angle when compared with the nonexchanged sample. Pb positions were found in the A channel close to M1, denoted Pb1, and M3, denoted Pb3, along with two new positions located off the mirror plane, Pb4 and Pb5 (Table 5 and Fig. 1). Because of space-group reduction from *C2/m* to *Cm*, the new sites Pb1' and Pb3' occur. In the other two structures, they were related by a center of symmetry. In the B channel, only one of the M2 sites, Pb2, is occupied.

Pb1 and Pb1' are sixfold coordinated to four framework O atoms and two channel H<sub>2</sub>O molecules [Pb1: 2 × O2 (2.86 Å), 2 × O3 (3.03 Å), O16 (2.73 Å), and O27 (2.40 Å); Pb1': 2 × O2' (2.77 Å), 2 × O3' (3.06 Å), O16' (2.39 Å), and O27' (2.56 Å)]. Pb2 is sixfold coordinated by 2 × O10 (2.76 Å) and O1' (2.64 Å) from the framework and three channel H<sub>2</sub>O molecules, 2 × O13 (2.44 Å) and O14 (2.65 Å) (Figs. 1 and 2). Pb3 (or Pb3') is close to Pb1 (or Pb1') and is surrounded by 2 × O2 (3.08 Å) [Pb3': 2 × O2' (3.05 Å)] and 2 × O3 (2.76 Å) [Pb3': 2 × O3' (2.77 Å)] from the framework and by channel H<sub>2</sub>O O28 (2.51 Å) [Pb3': O16' (2.37 Å)]. The channel H<sub>2</sub>O sites O27 and O27' are close to Pb3 (1.00 Å) and Pb3' (1.28 Å) and occur in the presence of Pb vacancies on Pb3 or Pb3' and coordinate Pb1 and Pb1'. Pb4 is coordinated by O6 (2.98 Å) and O6' (3.15 Å) from the framework and the channel H<sub>2</sub>O molecule O22 (2.70 Å). Pb5 has long distances (>3 Å) to framework O7, O7', O3, and O3' and to two channel H<sub>2</sub>O molecules, O16 (2.99 Å) and O16' (3.03 Å).

All Pb sites are only partially populated (Table 7). The localized concentration of Pb (4.00 Pb pfu) in the structural channels is in fair agreement with the Pb content determined by microprobe analysis (4.4 Pb pfu). The remaining 0.4 Pb pfu were not localized. However, some low Pb concentration may occupy what were refined as

channel H<sub>2</sub>O sites (O16, O16', O22, O27, O27', and O28), but these sparsely populated metal positions cannot be easily resolved from H<sub>2</sub>O.

The reason that the Pb-exchanged heulandite has an acentric space group, in contrast to the natural and Na-exchanged samples, is not understood yet. There seem to be two possibilities: (1) The acentricity is due to Si,Al ordering in the tetrahedral framework structure, and the Pb-H<sub>2</sub>O channel filling adopts the prescribed symmetry. In the view of the T-O distances, however, the structure refinement yielded a pseudocentric Si,Al distribution. (2) A preferred orientation of Pb-H<sub>2</sub>O clusters in the channels of a centric host structure is responsible for the acentric space group. However, why should parallel B channels, which are not even fully occupied, have the same Pb-H<sub>2</sub>O orientation and not an opposite arrangement that would introduce a center of symmetry?

In contrast to Na- or Ca-rich heulandite, the Pb-exchanged sample is ideal for studying acentricity with X-ray methods because Pb has a high anomalous dispersion contribution for MoK $\alpha$  X-radiation, which leads to significant differences between a centric and an acentric refinement model. Acentricity could also be present in non-exchanged and Na-exchanged heulandite samples but cannot be resolved from corresponding X-ray data.

### Optical properties

Electron microprobe analyses showed that the Poona sample was completely Na and Pb exchanged, but the Fiesch and Succor Creek samples were only partially Na and Pb exchanged. Optical properties (principal refractive indices,  $2V$ , and optical orientation) were determined for the nonexchanged, Na-, and Pb-exchanged Poona samples (Table 1). Refractive indices decreased for the Na-exchanged sample [mean refractive index ( $n$ ) = 1.4876] when compared with the nonexchanged sample (mean  $n$  = 1.5009), and refractive indices significantly increased for the Pb-exchanged sample (mean  $n$  = 1.5734). The trend of increasing mean  $n$  is similar to that found in the natrolite-group zeolites (Gunter and Ribbe, 1993). The Na end-member (natrolite) had the lowest value, and the Ca end-member (scolecite) had the highest value, and mesolite, containing both Na and Ca, was intermediate. This increase in mean  $n$  is related to both the H<sub>2</sub>O and cation content of the channels.

Zeolites commonly have low birefringence because they are framework structures (Gunter and Ribbe, 1989). Heulandite-group zeolites have perfect (010) cleavage, and the retardation is easy to observe in this orientation. The optical orientation (Table 1) remains basically unchanged for the three samples, with  $\mathbf{b} = Z$  yielding  $\delta_{010} = (\beta - \alpha)$ . The birefringence for the Poona sample changes dramatically after Pb exchange. The nonexchanged Poona  $\delta_{010}$  is 0.0010 (Fig. 3A), Na-exchanged = 0.0026, and Pb-exchanged = 0.0145 (Fig. 3B). A possible explanation for the high  $\delta$  in the Pb-exchanged sample can be found in the orientation of the framework O atoms and channel

H<sub>2</sub>O bonds to Pb2 (Fig. 2). The Pb2-O1 bond lies in (010) and is nearly parallel to  $Y$ , causing  $\beta$  to increase, thus causing the difference between  $\beta$  and  $\alpha$  to increase. In a similar manner to birefringence,  $2V$  varies for the three samples. The nonexchanged sample is optically positive with a  $2V_z$  value of 48.8°, whereas the Na-exchanged sample is negative with a  $2V_z$  value of 97.6°, and the Pb-exchanged sample has yet a larger negative  $2V_z$  value of 116.3°.

Boles (1972) and Gottardi and Galli (1985) noted the changes in optical orientation for clinoptilolite ( $\mathbf{b} = Y$ ) and heulandite ( $\mathbf{b} = Z$ ). Changes in optical orientation for the natrolite group were structurally related by Gunter and Ribbe (1993). For the natrolite group, only the channel contents change; the amount of Al and Si stay the same. Thus, changes in optical properties can be related to the amount and orientation of channel occupants. For heulandite-group zeolites, changes occur in the channel occupants (cations and H<sub>2</sub>O) and in the framework (the ratio of Al to Si). Boles (1972) observed how optical properties can be used to differentiate between clinoptilolite and heulandite. He found that when heulandite-group zeolites have a mean  $n < 1.482$ , it implies a channel cation occupancy with  $(\text{Na} + \text{K}) > \text{Ca}$ , which defines clinoptilolite (Mason and Sand, 1960), and a mean  $n > 1.494$  implies channel cation occupancy, which defines heulandite. It could be postulated that completely Na-exchanged heulandite would have optical properties similar to that of clinoptilolite. Interestingly, our Na-exchanged heulandite sample has a mean  $n$  of 1.488, placing it between the two end-members. Also, the optical orientation (i.e.,  $\mathbf{b} = Z$ ) remains the same for the Na-exchanged sample. This implies that the framework—changes in the Si-Al ratio or Si-Al ordering—has a significant effect on the optical orientation.

After the Pb-exchanged sample had been exposed to MoK $\alpha$  radiation for 1 week during the optical orientation measurement, the crystal was reexamined with a microscope equipped with a spindle stage. The crystal had become brownish during the X-ray exposure. Not only did the crystal suffer radiation-induced coloring but it also became pleochroic (pleochroic formula:  $X = \text{brown}$ ,  $Y = \text{light brown}$ , and  $Z = \text{clear}$ , which yields an absorption formula of  $X > Y > Z$ ). All of the other radiated Poona samples were clear. Before the crystal was irradiated,  $2V$  was determined;  $2V$  was again determined after irradiation and did not change. The mechanism for this radiation-induced pleochroism is still under study.

### Cation diffusion

After fully characterizing the Poona sample, we became interested in Pb diffusion into the other samples, and we wondered why only the Poona sample exchanged fully. Attempts were made to find some structural or chemical differences between these samples. These efforts so far have failed. It is possible that given longer exchange times the other two samples may have exchanged; thus, only

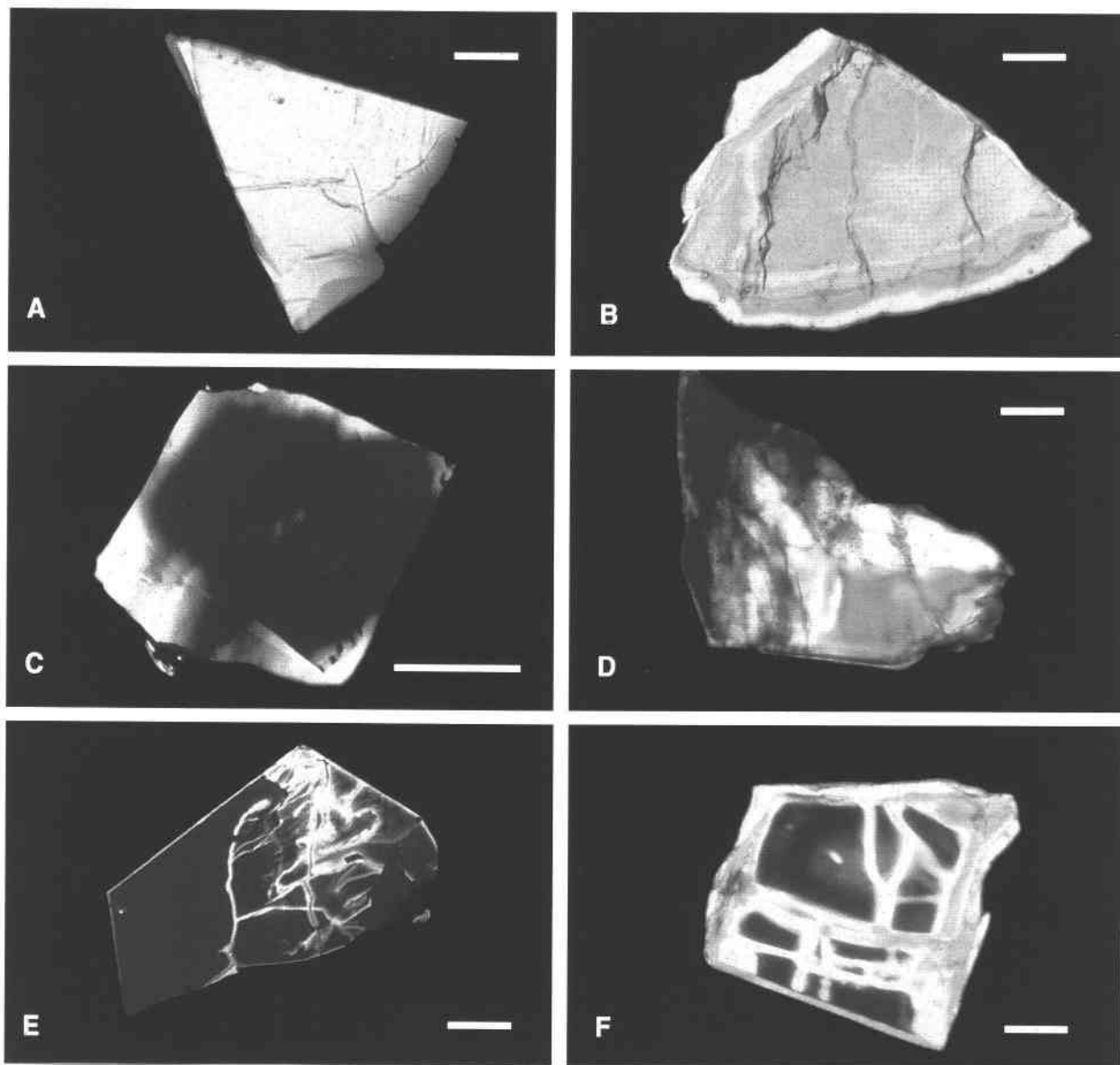


Fig. 3. Photomicrographs and BSE images for nonexchanged and Pb-exchanged heulandite-group zeolites (all scale bars are 100  $\mu\text{m}$ ; all photomicrographs are taken in cross-polarized light). (A) Photomicrograph of the nonexchanged Poona sample showing first-order gray retardation. (B) Photomicrograph of the fully Pb-exchanged Poona sample showing an increase in retardation to second-order red from first-order gray shown in A. This change in retardation is directly associated with the increase in birefringence ( $\beta - \alpha$ ) from 0.0010 (nonexchanged) to 0.0145 (Pb-exchanged). The decrease in retardation from the grain's center to its edge is associated with its decrease in thickness toward the edge and not a variation in Pb content. (C) BSE image of the partially Pb-exchanged Succor Creek sample showing how Pb, whose distribution is represented by the brighter areas, only dif-

fused around the grain's edge, approximately 10–50  $\mu\text{m}$ . (D) Photomicrograph of the partially Pb-exchanged Succor Creek sample showing how the retardation colors increased from first-order gray to first-order yellow in the lower right portion of the grain and to second-order blue in the extreme lower right portion of the grain (retardation increases from the nonexchanged core to the Pb-exchanged rim). In the upper central portion of the grain, no exchange occurred, and the grain is still first-order gray. (E) BSE image of the partially Pb-exchanged Fiesch sample showing Pb exchange along grain cracks and around the rim, producing the lighter areas in the photo. (F) Photomicrograph of the partially Pb-exchanged Fiesch sample showing how retardation colors have increased along the cracks and rim where Pb exchange has occurred.

the rate of exchange and not the ability to exchange may differ between the three samples. Research is underway to answer this question.

To gain a better understanding of cation diffusion rates into the partially exchanged samples from Fiesch and Succor Creek, BSE photos were taken, which showed that cation exchange occurred around the rims, ranging from 10 to 50  $\mu\text{m}$ , and along cracks (Fig. 3C and 3E). Because there is a significant change in the birefringence for the Pb-exchanged samples (compare Fig. 3A with Fig. 3B), an easily observable change in retardation results. Thus, the BSE photo of the Succor Creek sample shows Pb diffusing around the edge (Fig. 3C), whereas the photomicrograph shows changes in retardation and a diffusion gradient based on the retardation (Fig. 3D). BSE and photomicrographs of the Fiesch Pb-exchanged samples show much the same phenomenon, except exchange occurs in cracks as well as along the rims of the crystal (Fig. 3E and 3F).

#### ACKNOWLEDGMENTS

M.E.G. wishes to thank the Laboratorium für chemische und mineralogische Kristallographie, Universität Bern, and the National Science Foundation (NSF-INT 9123567) for financial support to perform this study.

#### REFERENCES CITED

- Alberti, A. (1972) On the crystal structure of the zeolite heulandite. *Tschermaks mineralogische und Petrographische Mitteilungen*, 18, 129–146.
- (1975) The crystal structures of two clinoptilolites. *Tschermaks mineralogische und Petrographische Mitteilungen*, 22, 25–37.
- Armbruster, Th., and Gunter, M.E. (1991) Stepwise dehydration of a heulandite-clinoptilolite from Succor Creek, Oregon, U.S.A.: A single crystal X-ray study at 100 K. *American Mineralogist*, 76, 1872–1883.
- Blanchard, G., Maunay, M., and Martin, G. (1984) Removal of heavy metals from waters by means of natural zeolites. *Water Research*, 18, 1501–1507.
- Bloss, F.D. (1981) *The spindle stage: Principles and practice*, 340 p. Cambridge University Press, Cambridge, U.K.
- Boles, J.R. (1972) Composition, optical properties, cell dimensions, and thermal stability of some heulandite-group zeolites. *American Mineralogist*, 57, 1452–1493.
- Bresciani-Pahor, N., Calligaris, M., Nardin, G., Randaccio, L., Russo, E., and Comin-Chiaromonti, P. (1980) Crystal structure of a natural and a partially silver-exchanged heulandite. *Journal of the Chemical Society, Dalton Transactions*, 1511–1514.
- Bresciani-Pahor, N., Calligaris, M., Nardin, G., and Randaccio, L. (1981) Location of cations in metal ion-exchanged zeolites. II. Crystal structures of a fully silver-exchanged heulandite. *Journal of the Chemical Society, Dalton Transactions*, 2288–2291.
- Enraf-Nonius (1983) Structure determination package (SDP). Enraf-Nonius, Delft, The Netherlands.
- Galli, E., Gottardi, G., Mayer, H., Preisinger, A., and Passaglia, E. (1983) The structure of a potassium-exchanged heulandite at 293, 373 and 593 K. *Acta Crystallographica*, B39, 189–197.
- Gottardi, G., and Galli, D. (1985) *Natural zeolites*, 409 p. Springer-Verlag, Berlin.
- Grube, W.E., Jr., and Herrmann, J.G. (1993) Heavy metal fixation by natural zeolite. Fourth International Conference on the Occurrence, Properties, and Utilization of Natural Zeolites, Boise, Idaho, 112–114.
- Gunter, M.E., and Ribbe, P.H. (1989) Zeolites: Structural and chemical interpretations of optical properties. *Geological Society of America Abstracts with Programs*, 21 (6), 117–118.
- (1993) Natrolite group zeolites: Correlations of optical properties and crystal chemistry. *Zeolites*, 13, 435–440.
- Gunter, M.E., Bloss, F.D., and Su, S.C. (1988) EXCALIBUR revisited. *American Mineralogist*, 73, 1481–1482.
- Koyama, K., and Takéuchi, Y. (1977) Clinoptilolite: The distribution of potassium atoms and its role in thermal stability. *Zeitschrift für Kristallographie*, 145, 216–239.
- Leppert, D. (1990) Heavy metal sorption with clinoptilolite zeolite: Alternatives for treating contaminated soil and water. *Mining Engineering*, 42 (6), 604–608.
- Mason, B., and Sand, L.B. (1960) Clinoptilolite from Patagonia: The relationship between clinoptilolite and heulandite. *American Mineralogist*, 45, 341–350.
- Merkle, A.B., and Slaughter, M. (1968) Determination and refinement of the structure of heulandite. *American Mineralogist*, 53, 1120–1138.
- Mortier, W.J., and Pearce, J.R. (1981) Thermal stability of the heulandite-type framework: Crystal structure of the calcium/ammonium form dehydrated at 483 K. *American Mineralogist*, 66, 309–314.
- Mumpton, F.A. (1960) Clinoptilolite redefined. *American Mineralogist*, 45, 351–369.
- (1978) Natural zeolites: A new industrial mineral commodity. In L.B. Sand and F.A. Mumpton, Eds., *Natural zeolites: Occurrence, properties, use*, p. 3–27. Pergamon, New York.
- (1988) Development of uses for natural zeolites: A critical commentary. In D. Kallo and H.S. Sherry, Eds., *Occurrence, properties, and utilization of natural zeolites*, p. 333–365. Akademiai Kiado, Budapest.
- Petrov, O.E., Filizova, G., and Kirov, N. (1991) Cation distribution in clinoptilolite structure: Cs-exchanged sample. *Comptes rendus de l'Académie Bulgare des Sciences*, 44, 77–80.
- Pond, W.G., Ellis, K.J., Krook, L.P., and Schoknecht, P.A. (1993) Modulation of dietary lead toxicity in pigs by clinoptilolite. Fourth International Conference on the Occurrence, Properties, and Utilization of Natural Zeolites, Boise, Idaho, 170–172.
- Sheldrick, G.M. (1976) SHELX76. Program for crystal structure determination. University of Cambridge, Cambridge, England.
- Smith, J.V., Pluth, J.J., Artioli, G., and Ross, F.K. (1984) Neutron and x-ray refinements of scolecite. In A. Bisio and D.H. Olson, Eds., *Proceedings of the 6th International zeolite conference*, p. 842–850. Butterworths, Guildford, U.K.
- Smyth, J.R., Spaid, A.T., and Bish, D.L. (1990) Crystal structures of a natural and a Cs-exchanged clinoptilolite. *American Mineralogist*, 75, 522–528.
- Stuckenschmidt, E., Joswig, W., and Baur, W.H. (1993) Natrolite. I. Refinement of high-order data, separation of internal and external vibration amplitudes from displacement parameters. *Physics and Chemistry of Minerals*, 19, 562–570.
- Su, S.C., Bloss, F.D., and Gunter, M.E. (1987) Procedures and computer programs to refine the double variation method. *American Mineralogist*, 72, 1011–1013.
- Sugiyama, K., and Takéuchi, Y. (1986) Distribution of cations and water molecules in the heulandite-type framework. *Studies in Surface Science and Catalysis*, 28, 449–456.
- Sukheswala, R.N., Avasia, R.K., and Gangopadhyay, M. (1974) Zeolites and associated secondary minerals in the Deccan Traps of western India. *Mineralogical Magazine*, 39, 658–671.
- Tiselius, A. (1934) Die Diffusion von Wasser in einem Zeolithkristall. *Zeitschrift für Physikalische Chemie*, 169A, 425–458.
- Tschernich, R.W. (1992) *Zeolites of the world*, 563 p. Geoscience, Phoenix, Arizona.
- Tuck, L.K., and Ming, D.W. (1993) Adsorption of cadmium and lead by clay-liner material amended with clinoptilolite. Fourth International Conference on the Occurrence, Properties, and Utilization of Natural Zeolites, Boise, Idaho, 205–207.

MANUSCRIPT RECEIVED OCTOBER 1, 1993

MANUSCRIPT ACCEPTED MARCH 2, 1994